Published in final edited form as:
Gene Ther. 2014 May ; 21(5): 507–513. doi:10.1038/gt.2014.24.

AAV Mediated Expression of Human PRELP inhibits Complement Activation, Choroidal Neovascularization and Deposition of Membrane Attack Complex in Mice

Marco T. Birke, **Erion Lipo**, **Mehreen Adhi**, **Kerstin Birke**, and **Rajendra Kumar-Singh***
Department of Ophthalmology, Tufts University School of Medicine, 136 Harrison Avenue, Boston, MA 02111, USA

Abstract

Age related macular degeneration (AMD) is the leading cause of blindness among the elderly. Approximately 50% of AMD patients have a polymorphism in the negative regulator of complement known as Factor H. Individuals homozygous for a Y402H polymorphism in Factor H have elevated levels of membrane attack complex (MAC) in their choroid and retinal pigment epithelium relative to individuals homozygous for the wild type allele. An inability to form MAC due to a polymorphism in C9 is protective against the formation of choroidal neovascularization (CNV) in AMD patients. Hence, blocking MAC in AMD patients may be protective against CNV. Here we investigate the potential of human proline/arginine-rich end leucine-rich repeat protein (PRELP) as an inhibitor of complement mediated damage when delivered via the subretinal route using an AAV2/8 vector. In a FACS lysis assay, PRELP inhibited normal human serum mediated lysis of Hepa-1c1c7 cells by 18.7%. Unexpectedly, PRELP enhanced the formation of tubes by HUVECs by approximately 240% but when delivered via an AAV vector to the retina of mice, PRELP inhibited laser induced CNV by 60%. PRELP reduced deposition of MAC *in vivo* by 25.5%. Our results have implications for the development of complement inhibitors as a therapy for AMD.

Keywords

age related macular degeneration (AMD); proline/arginine-rich end leucine-rich repeat protein (PRELP); complement system; membrane attack complex (MAC)

Introduction

Age related macular degeneration (AMD) is the leading cause of blindness among the elderly, affecting approximately 1 in 3 people over the age of 70 [1]. Approximately 90% of AMD patients suffer from the ‘dry’ or non-exudative form of AMD. The remaining patients suffer from ‘wet’ or exudative AMD, involving the growth of new blood vessels from the

***Correspondence should be addressed to**Rajendra.Kumar-Singh@tufts.edu.

Conflict of Interest
The authors do not have any conflicts of interest to declare.

Supplementary information **is available at Gene Therapy’s website.**

choroid into the subretinal space, i.e. choroidal neovascularization (CNV) [2]. Whereas 'wet' AMD may be treated with anti-vascular endothelial growth factor (VEGF) molecules, there are currently no treatment options for 'dry' AMD. In general, 'dry' AMD progresses to 'wet' AMD in 10% of patients but both forms of the disease can also exist concomitantly. Although the cause of AMD is not well understood, significant evidence has accumulated that complement plays a key role in the disease process [3]. For example, 50% of AMD patients have a polymorphism in the complement regulator Factor H with a common Y402H variant present in approximately 43% of AMD patients [4]. Activation of complement terminates in the formation of a pore known as the membrane attack complex (MAC) on the surface of pathogens and host tissues [5]. Low levels of MAC on host tissues lead to an elevation of cytokines such as VEGF [6] and high levels of MAC lead to cell lysis [7]. Damage to host tissues is prevented by the expression of regulators of complement such as CD59 and CD46 [8]. Advanced AMD patients have reduced levels of CD59 and CD46 on their RPE cells [9] and loss of RPE cells is a hallmark of advanced AMD known as geographic atrophy [3]. Individuals homozygous for the Y402H polymorphism in Factor H have approximately 70% more MAC on their choroidal blood vessels, RPE and the associated Bruch's membrane [3]. An inability to form MAC by virtue of a polymorphism in C9, an essential protein for the formation of MAC, protects individuals from the development of 'wet' AMD [10].

Notably, Factor H with a Y402H polymorphism binds less efficiently to heparan sulfate and dermatan sulfate glycosaminoglycans within Bruch's membrane than wild-type (WT) Factor H [11]. Based on the above collective observations, a model is emerging that suggests an imbalance between complement activation and complement inhibition may play a significant role in the pathogenesis of AMD. We postulate that inhibition of local complement activation and particularly inhibition of MAC deposition on host tissues may protect against the conversion of 'dry' to 'wet' AMD.

PRELP (proline/arginine-rich end leucine-rich repeat protein) is an aproximately 42 to 58 kDa extracellular matrix protein [12-16] found in connective tissues such as sclera, tendon, skin, lung and heart [13, 15]. The N terminus of PRELP has been shown to bind both heparin and heparan sulfate proteoglycans in the extracellular matrix [17]. PRELP also binds perlecan, a component of the Bruch's membrane [18]. PRELP is a recently identified inhibitor of C9 polymerization [14], a process necessary for assembly of the MAC [19]. PRELP also interacts with C3 and different polymorphisms in C3 have been shown to promote or reduce the risk of AMD [20, 21]. To date, the anti-complement activities of PRELP have not been investigated *in vivo*.

The most commonly used model of 'wet' AMD is laser induced CNV [22, 23]. In this model, a laser is utilized to disrupt the Bruch's membrane, which leads to an elevation of cytokines such as VEGF and subsequent development of CNV. This model has been widely used to measure the efficacy of inhibitors of angiogenesis and particularly CNV [22-24]. In addition to the process of CNV, in this model there is deposition of MAC at the site of the laser burn [25]. Hence, while this model has some limitations as a true model for 'wet' AMD, it is an ideal model to test the efficacy of inhibitors of CNV and MAC. In this study we test the hypothesis that expression of human PRELP in murine retina via an adeno-associated virus

(AAV) vector attenuates the progression of laser induced CNV and deposition of the MAC. Our results have potential implications for the future development of anti-complement therapies for AMD.

Results

PRELP Inhibits Normal Human Serum Mediated Cell Lysis

In order to determine whether PRELP may protect cells from complement mediated cell lysis, we constructed a plasmid containing an expression cassette expressing the human PRELP cDNA regulated by the CMV enhancer/chicken β-actin promoter and a rabbit globin poly adenylation (pA) signal. As we wished to ultimately express PRELP *in vivo*, we flanked the PRELP expression cassette with adeno-associated virus serotype 2 (AAV2) inverted terminal repeats (pAAV2-PRELP, Figure 1A). As a negative control, we constructed a similar plasmid devoid of the PRELP cDNA (pAAV2-pA, Figure 1A). Western blot analyses of media from human ARPE-19 cells transfected with pAAV2-PRELP indicated an immunostained protein band of approximately 44 kDa, consistent with the predicted molecular weight of 43.84 kDa (http://www.bioinformatics.org/sms2/protein_mw.html) of human PRELP (Figure 1B). As expected, this band was absent in samples containing media from ARPE-19 cells transfected with pAAV2-pA (Figure 1B).

In a standard FACS lysis assay, a total of 90.16±1.09% of murine Hepa-1c1c7 cells incubated in 1.5% normal human serum (NHS) were lysed by NHS pre-conditioned with media from human ARPE-19 cells transfected with pAAV2-pA (Figure 1C, 1D). In contrast, a total of 71.42±3.79% of Hepa-1c1c7 cells incubated in 1.5% NHS were lysed when the NHS was pre-conditioned with media from human ARPE-19 cells transfected with pAAV2-PRELP (Figure 1C, 1D), corresponding to an approximately 18.74±3.95% (*p=0.0015)* reduction in PRELP mediated cell lysis. In conclusion, we show that PRELP significantly inhibits NHS mediated cell lysis of Hepa-1c1c7 cells.

Human PRELP Promotes Formation of Tubes by HUVECs

Endothelial cell migration and subsequent formation of tubes is a generally accepted prerequisite of angiogenesis. New blood vessels formed in ‘wet’ AMD leak blood and plasma to form a macular edema. VEGF is a vascular permeability factor and the occurrence of macular edema is associated with elevated VEGF. One commonly used standard assay to measure the potency of inhibitors of tube formation involve the counting of master junctions, master segments or meshes formed by human umbilical vein endothelial cells (HUVECs) in the presence or absence of a reagent predicted to attenuate tube formation. Hence, we incubated HUVEC cells with a commercially available mix of growth factors that activate and promote the formation of tubes by HUVECs and supplemented this mix with either media from pAAV2-PRELP transfected ARPE-19 cells or media from pAAV2-pA transfected ARPE-19 cells. As a negative control, we included suramin, an inhibitor of HUVEC tube formation. Suramin completely blocked the formation of junctions, segments or meshes in these assays (data not shown). We found that HUVECs cultured pA preconditioned medium formed an average of 8.52±1.22 master junctions/ mm^2, 14.10±2.17 master segments/ mm^2 and 4.44±0.88 meshes/ mm^2 respectively (Fig. 2A, B). In contrast,

HUVECs cultured in PRELP preconditioned medium formed an average of 18.24±0.95 master junctions/ mm^2, 32.26±1.79 master segments/ mm^2 and 12.88±0.92 meshes/ mm^2 respectively (Fig. 2A, B). Contrary to our expectations, our data indicated that there was a 2.1-fold *increase* in the formation of master junctions ($p<0.0001$), a 2.3-fold *increase* in the formation of master segments ($p<0.0001$) and a 2.9-fold *increase* in formation of meshes ($p<0.0001$) respectively when HUVECs are incubated in pAAV2-PRELP conditioned media relative to pAAV2-pA conditioned media. We conclude that expression of human PRELP *enhanced* the formation of tubes by HUVECs. Nonetheless, since HUVECs are not a surrogate for *in vivo* studies and choroidal endothelial cells in culture would not necessarily predict the outcomes of endothelial cells *in vivo*, we proceeded to evaluate the activity of human PRELP *in vivo*.

Expression of human PRELP in murine retina

AAV vectors are efficient gene delivery vehicles for the murine and human retina [26]. In order to deliver the PRELP cDNA to the murine retina, we utilized an AAV2/8-PRELP vector and an AAV2/8-pA vector as the corresponding negative control. To determine the localization of human PRELP following delivery to the murine retina, AAV2/8-PRELP or AAV2/8-pA were injected into the subretinal space of adult C57Bl/6J mice. Two weeks later, the mice were sacrificed and frozen retinal sections examined for expression of human PRELP by immunocytochemistry. Since PRELP is a secreted protein found in the extracellular matrix, we wished to distinguish PRELP localization independently of gene expression associated with the tropism of AAV2/8, i.e. we wished to distinguish regions of the retina that contained PRELP that had not been directly infected by the virus vector. Hence, prior to subretinal injection, the AAV2/8-PRELP or AAV2/8-pA virus preparations were ‘spiked’ with AAV2/8-GFP. We found that GFP in AAV2/8-PRELP injected eyes was present in the outer nuclear layer (ONL) and the retinal pigment epithelium (RPE) (Figure 3A). In these same sections, PRELP was found abundantly in the inner retina and outer segments but unexpectedly, not in the ONL (Figure 3B). AAV2/8-pA injected mice stained for human PRELP were negative as expected (Figure 3C) as were uninjected mice (Figure 3I). At higher magnification, we found that GFP was also present abundantly in the outer segments (Figure 3D) and that staining within the ONL was perinuclear (Figure 3D, F, G). An overlay of the GFP and Cy3 signal associated with PRELP staining (yellow), indicated areas of overlap but also areas of clear distinction between GFP expression and localization of PRELP (Figure 3F). These data suggest that following subretinal injection, PRELP is synthesized in the photoreceptors and RPE and thereafter secreted. PRELP subsequently localizes to the inner retina as well as the outer retina except in the ONL. In contrast, GFP is present only in the photoreceptors and RPE, consistent with the presumed transduction pattern of AAV2/8-GFP.

Human PRELP Attenuates Choroidal Neovascularization in Mice

In order to determine whether human PRELP can attenuate laser induced CNV, AAV2/8-PRELP or AAV2/8-pA were injected into the subretinal space of 6 week old C57Bl/6J mice and 2 weeks later, 4 laser spots were created in the choroid equidistant from the optic nerve head. A further 7 days thereafter, mice were sacrificed and eyes harvested, stained with GSL-1 lectin (Figure 4A) and the area of CNV quantified using Image J Software. The

average area of CNV spot size in AAV2/8-pA injected eyes was found to be 3.025±0.355 $\times 10^4$ μm^2 (n=61 laser spots,10 mice/ 20 eyes). In contrast, the average area of CNV spot size in AAV2/8-PRELP injected eyes was 1.250±0.138 $\times 10^4$ μm^2 (n=55 laser spots), corresponding to a 60.0±13.1% (*p<0.0001*) reduction in laser induced CNV (Figure 4B). We conclude that human PRELP attenuates laser induced CNV in C57Bl/6J mice.

Human PRELP Attenuates Formation of Membrane Attack Complex in Mice

Formation of the membrane attack complex (MAC) begins with the incorporation of the C5b678 complex into the surface of cell membranes and followed by the recruitment and polymerization of multiple C9 units to form C5b9 [27]. In order to determine whether a reduction in CNV was associated with a reduction in MAC, we stained AAV2/8-PRELP injected eyes or AAV2/8-pA injected eyes with an antibody against C5b9. We found that for similar sized laser spots, C5b9 staining extended beyond the region of the GSL-1 stained CNV in AAV2/8-pA injected eyes (Figure 5A). In contrast, in AAV2/8-PRELP injected eyes, C5b9 staining did not extend beyond the GSL-1 stained CNV and staining was overall weaker within the CNV. Quantification of the signal intensity/area revealed an average ratio of 3.376±0.288 $\times 10^4$ u/ μm^2 in AAV2/8-pA injected eyes (n=61 laser spots, 10 mice/ 20 eyes) and of 2.516±0.300 $\times 10^4$ u/ μm^2 in AAV2/8-PRELP injected eyes (n=55 laser spots, 10 mice/ 20 eyes), corresponding to a significant reduction in MAC staining of approximately of 25.5±12.3% (*p=0.0409*; Fig. 5B). We conclude that human PRELP attenuates murine MAC deposition in laser induced CNV.

Discussion

In this study we report that human PRELP promotes the formation of tubes by HUVEC cells *in vitro*, yet inhibits angiogenesis and specifically choroidal neovascularization *in vivo*. We also report that human PRELP significantly inhibits NHS mediated lysis *in vitro* and inhibits formation of murine MAC *in vivo*. These results confirm a role for complement activation in laser induced CNV and confirm for the first time *in vivo*, the anti-complement activities of human PRELP. These studies shed further light on the functions of PRELP and have potential implications for the development of anti-complement therapies for AMD.

Although AMD is a complex disorder, significant evidence indicates that activation of complement plays a significant role in disease pathology. Balance between activation and inhibition of complement is maintained by a number of proteins. Polymorphisms in complement Factors/proteins H, C3, C2, C1, B, I, D, and C4 have been previously associated with AMD [3, 28, 29]. Polymorphisms in Factor H can be found in approximately 50% of AMD patients and homozygosity for a frequent Y402H polymorphism leads to an almost 70% increase in MAC deposition in the choroidal blood vessels, RPE and Bruch's membrane - the primary sites of pathology in AMD patients [3, 4, 28]. An inability to form MAC due to a polymorphism in C9 protects against wet AMD in humans [10]. Complement is also involved in tissue homeostasis, and particularly in angiogenesis, apoptosis, cytokine release and chemotaxis of macrophages [30] - all factors previously implicated in AMD [31, 32]. Hence, complement may play a role in the pathogenesis of AMD not only through MAC but also through its interactions with other key biological pathways. Based on these and

additional criteria, we were motivated to identify and test molecules that may inhibit complement activation and specifically CNV and MAC deposition in murine models of AMD.

In general, proteins that are found to be efficacious as inhibitors of angiogenesis or specifically CNV *in vivo*, also tend to function as inhibitors of endothelial tube formation *in vitro*. Hence, HUVEC cells in culture are often utilized as a surrogate for angiogenesis *in vivo*. Despite this, we were surprised to find that instead of *inhibiting* the formation of tubes by HUVECs, PRELP *enhanced* tube formation more than two fold. This observation could be explained by considering that the complement cascade plays a significant role in angiogenesis *in vivo* [33] but in the HUVEC tube formation assay *in vitro*, the complement cascade is largely absent and hence angiogenesis in the *in vitro* model is primarily driven by factors other than complement, such as cytokines. This hypothesis is also consistent with the knowledge that the extracellular matrix also plays a key role in angiognenesis *in vivo* [34] and cells in culture have a limited extracellular matrix relative to that *in vivo*. The N terminus of PRELP has been previously described to bind and localize to the extracellular matrix [17]. In our own studies, the immunostaining pattern for PRELP appeared to be extracellular (Figure 3E, F) relative to the expression of GFP that was primarily perinuclear in the ONL (Figure 3D, F, G) and nuclear and cytoplasmic in the RPE (Figure 3D, F, H).

The complement system can be activated through three different pathways, the classical, the lectin and the alternative pathway. These pathways converge into the terminal pathway that results in the deposition of MAC. PRELP interferes with the formation of MAC by inhibiting polymerization of C9, an essential component of MAC [14, 19]. PRELP also inhibits the alternative pathway of complement by inhibiting the formation of the C3-convertase C3bBbP [14]. Hence, PRELP may be acting at various stages of complement activation in order to reduce laser induced CNV and MAC deposition.

Previously we have described an AAV2 vector expressing human CD59 with a deletion in the GPI-anchor of CD59 (AAVCAGsCD59). Similar to PRELP, CD59 blocks the completion of the formation of MAC [30]. However, CD59 is not known to attenuate complement at additional stages of complement activation. Expression of CD59 on the RPE of advanced AMD patients is diminished relative to normal individuals and this may potentially expose the RPE cells to MAC associated lysis or cause an elevation in cytokine release through the deposition of MAC. While attenuation of complement at various stages of activation through the use of PRELP has its advantages in terms of potentially greater potency, it may also be disadvantageous given that complement plays various roles in tissue homeostasis [35]. In our studies involving AAVCAGsCD59 we found a 62% reduction in CNV [25] and 73% reduction in MAC respectively (our unpublished results). In the current study utilizing PRELP, we observed a comparable 60% reduction in CNV but a 25% reduction in MAC. However, these two studies cannot be directly compared because we utilized different serotypes of AAV vectors between the different studies as well as different modes of vector delivery to the eye. However, both studies corroborate that inhibition of complement and inhibition of MAC attenuates CNV. Thus far, these are the only studies utilizing a gene therapy approach for the inhibition of complement in animal models of AMD. Given that the AAV2 vector has been shown to be safe and persists long-term in

humans [36], and that AMD is a slow chronic disease, it is tempting to believe that a gene therapy approach to deliver inhibitors of complement to human eyes may be efficacious for the treatment of AMD.

Materials and Methods

Cell culture

Human umbilical vein endothelial cells (HUVEC; Life Technologies Corporation, Carlsbad, CA) were maintained in phenol red-free medium (200PRF; Life Technologies) supplemented with 2% Low Serum Growth Supplement (LSGS; Life Technologies). Mouse hepatoma cells (Hepa-1c1c7; ATCC, Manassas, VA) were maintained in Minimal Essential Medium (MEMa; Life Technologies) supplemented with 10% fetal bovine serum (FBS; Life Technologies). Human embryonic kidney cells (HEK-293, AAV-293; Stratagene, Santa Clara, CA) were cultured in Dulbecco's Modified Eagle Medium (DMEM; Life Technologies) supplemented with 10% FBS. Human retinal pigment epithelium cells (ARPE-19; CRL-2302; ATCC, Manassas, VA) were maintained in phenol red free DMEM/F-12 (Life Technologies) supplemented with 10% FBS. All cell lines were propagated at 37°C in a humidified 5% CO_2-air incubator.

Generation of AAV constructs

The coding sequence of human PRELP was amplified by PCR from IMAGE-clone 5222817 (MGC-45323; ATCC) using primers hPrelp fwd. (5′-GAATTCATGAGGTCACCCCTCTGCTG-3′) and hPrelp rev. (5′-CTCGAGCTAGATGACCACGGACTGCAG-3′). The PCR product was cloned in a pAAV2 vector containing a CMV enhancer /chicken β-actin promoter (CAG) to generate pAAV2-Prelp. The sequence of the cloned PCR product was verified by Tufts University Sequencing Core. AAV2/8 production and purification was performed as described previously [25]. Briefly, AAV-293 cells were triple transfected using $CaPO_4$ with pAAV2-Prelp, pHelper and replication/serotype 8 capsid-plasmid pRC/8 (Agilent Technologies, Santa Clara, CA). PEG-precipitated medium/cell lysate mixtures were purified by high-speed IDX-density-gradient centrifugation and concentrated with sepharose spin-columns. Purity of viruses was assessed in silver-stained polyacrylamide gels indicating major proteins corresponding to AAV8 VP1 (87kDa), VP2 (72kDa) and VP3 (62kDa) as expected (supplemental Fig. 1). Virus titers were determined by AAV2-specific real-time PCR quantification of virus genomes as described previously [37]. AAV2/8-pA control virus was generated in a similar fashion. Western blot analyses of media from ARPE-19 cells infected with AAV2/8-PRELP indicated a unique band at approximately 44kDa as expected, which was absent in the media of ARPE-19 cells infected with AAV2/8-pA or another negative control vector expressing green fluorescent protein (AAV2/8-GFP, supplemental Fig. 1).

Generation of PRELP conditioned ARPE-19 medium

ARPE-19 were $CaPO_4$-transfected with pAAV2-PRELP or pAAV2-pA to produce conditioned medium. Protein expression was extended for 72h after transfection in serum-free medium. For protein extraction, cells were scratched from the plates and sheared by repeated aspiration/expiration through a 25G needle to liberate the cell contents into the

surrounding culture medium. Medium/lysate mixtures were cleared from cellular debris by centrifugation. Media-supernatants were designated as 'PRELP-conditioned medium' or 'pA-conditioned medium' for subsequent *in vitro* studies and stored at −80°C in 1mL aliquots.

AAV2/8 infection of ARPE-19 Cells

ARPE-19 were infected with multiplicity of infection (MOI) of 20,000 with AAV2/8-PRELP or AAV2/8-pA for 72h. Extraction and purification was performed as described for conditioned medium. Supernatants (ARPE-19:AAV2/8-PRELP, ARPE-19:AAV2/8/pA) were stored at −80°C in 1mL aliquots.

Western Blot Analyses

Denatured and reduced samples were separated by standard 10% SDS-PAGE and transferred onto a nitrocellulose membrane by tank-blot (BioRAD). Detection was performed according to the LI-COR®-Odyssey protocol (LI-COR® Biosciences, Lincoln, NE). In brief, membranes were blocked in LI-COR® blocking solution, a rabbit-polyclonal-anti-hPRELP antibody (SAB1100370; Sigma-Aldrich, St. Louis, MO) diluted 1:250 in 1:1 (v/v) blocking solution/ PBST (PBS/ 0.1% tween-20) was added and detected with a goat-anti-rabbit-IRDye®800CW antibody (1:15,000 in 1:1 blocking solution/PBST; LI-COR® Biosciences).

Normal human serum (NHS) mediated cell lysis assay

FACS lysis assays were performed as previously described [25]. In brief, 5.0×10^4 Hepa-1c1c7 cells per assay were resuspended in either PRELP- or pA-conditioned medium. NHS was added to 1.5%. Cells were allowed to react for one hour at 37°C with constant gentle rotary motion. Cell lysis was measured as uptake of propidium iodide in 2.5×10^4 cells by flow cytometry (FACSCalibur, Becton Dickinson). Quantification and analyses were performed with the FlowJo software (Tree Star Inc., Ashland, OR).

HUVEC Tube Formation Assay

Tube formation assays were carried out according to the Endothelial Tube Formation Assay (In vitro Angiogenesis) protocol (Life Technologies). Briefly, 4.5×10^4 HUVECs per assay were seeded in either PRELP- or pA-conditioned medium on Geltrex™ (Reduced Growth Factor Basement Membrane Matrix; Life Technologies) coated wells of a 24-well plate. Tube formation was induced with 2% Low Serum Growth Supplement (LSGS). Cells were analyzed after 16-20h under an inverted microscope (IX51; Olympus) and images captured. Numbers of master junctions, master segments and meshes in each image were quantified using the "HUVEC angiogenesis analyzer" plugin for the ImageJ software.

Animals

This study was carried out in strict accordance with the Statement for the Use of Animals in Ophthalmic and Vision Research, set out by the Association of Research in Vision and Ophthalmology (ARVO) and was approved by Tufts University Institutional Animal Care and Use Committee (IACUC) protocol B2011-150 and Tufts University Institutional

Biosafety Committee registration 2011-BRIA68. For experiments 6 weeks old C57Bl/6J mice (Jackson laboratory, Bar Harbor, ME) were used. Animals were anesthetized by intraperitoneal injections of a mixture containing 0.1mg/g body weight Ketamine (Phoenix™, St Joseph, MO) and of 0.01mg/g body weight Xylazine (Lloyed, Shenandoah, IA). Mice were kept warm during anesthesia. Mice were sacrificed by CO_2 inhalation followed by cervical dislocation.

Subretinal injections

Subretinal injections were performed as previously described [25]. In brief, 2.8×10^{10} genome copies of AAV2/8-PRELP were delivered in a total volume of 1μl by a trans-scleral/ trans-choroidal approach with a 32G needle attached to a 5μl glass syringe (Hamilton, Reno, NV). PRELP virus was injected in both eyes of mice (n=10 mice, 20 eyes). The corresponding control cohort was injected with AAV2/8-pA following the same protocol.

Posterior eyecup labeling

Localization of PRELP in the posterior eye was determined 2 weeks after injection. Mice were sacrificed, eyes enucleated, opened by a transcorneal punch and fixed by immersion in 4% PFA in toto. Eyes were dehydrated in 15% and 30% sucrose, cornea and lens removed and specimens embedded in Tissue-Tek® Cryo-O.C.T.™ Compound (Electron Microscopy Sciences, Hatfield, PA). 12μm thick sections were made on a cryostat (Microm HM550) and dried onto microscope slides. Sections were blocked in PBS/6% NGS/0.1% TritonX-100, labeled with a rabbit-polyclonal-anti-hPRELP antibody (1:250 in blocking solution; SAB1100370, Sigma-Aldrich) and detected with a Cy3 conjugated goat-anti-rabbit antibody (1:400 in PBST; Jackson ImmunoResearch Laboratories). Nuclei were counterstained with DAPI.

For detection of CNV area and MAC, mice were sacrificed seven days after lasering and the eyes enucleated. Cornea, iris, lens and the neuronal retina were removed and posterior eye segments fixed by immersion in 4% PFA. RPE/choroid specimens were cut four times from the edge to the center to obtain trefoil shaped flatmounts. After blocking in PBS/2.5 mg/ml BSA, flatmounts were stained with FITC-conjugated Griffonia Simplicifolia Lectin I (GSL I, isolectin B4; 10mg/ml in PBS; Vector Labs). Specimens were washed with PBS, re-blocked with 6% normal goat serum (NGS; Jackson ImmunoResearch Laboratories, West Grove, PA) in PBS/0.3% TritonX-100 (PBST) and labeled with a rabbit-anti-hC5b9 antibody (1:200 in PBST; Complement Technology, Inc., Tyler, TX). Detection was done with a Cy3-conjugated goat-anti-rabbit antibody (1:400 in PBST; Jackson ImmunoResearch Laboratories). Flat mounts were analyzed under an inverted microscope (IX51; Olympus, Center Valley, PA) attached to a fluorescence unit and images captured. Areas of GSL-I labeling (CNV areas), size and signal intensities of C5b9 labeled areas (MAC areas) were measured using ImageJ software (http://rsbweb.nih.gov/ij/). Data points for MAC deposition are depicted as C5b9 intensities per C5b9 area ratios. C5b9 intensities were corrected for background intensities before calculations. Area and intensity measurements were analyzed with GraphPad Prism6 (GraphPad Software, La Jolla, CA) using an unpaired student's t-test. All data is presented as Mean±SEM.

Laser induced choroidal neovascularization (CNV)

Laser induced choroidal neo-vascularization was performed as described previously [25]. Briefly, pupils of anesthetized mice were dilated with one drop each of 2.5% phenylephrine HCl and 1% Tropicamide (Bausch & Lomb Incorporate, Tampa, FL). The cornea was protected with one drop of 2.5% Hypromellose (Goniovisc, Wellhead, UK) and a cover slip. Four laser spots around the optic nerve head were generated per eye with an argon laser (532nm; IRIS Medical Light solutions, IRIDEM, IRIDEX, Mountain View, CA). The settings were 75μm spot size, 100ms pulse time, 150mW power.

Statistical Analysis

Statistical analysis was performed using the GraphPad Prism6 software (GraphPad Software, La Jolla, CA). Significance of differences were determined by an unpaired student's t-test. For each *in vivo* experiment 5 mice per group were utilized. *In vitro* experiments were performed in duplicate. All experiments were repeated at least three times. All data are presented as mean±SEM.

Supplementary Material

Refer to Web version on PubMed Central for supplementary material.

Acknowledgments

This study was supported by grants to R.K.S from The Ellison Foundation, The Virginia B Smith Trust, The National Institute of Health/NEI (EY021805 and EY013837), The Department of Defense/ TATRC, The Paul and Phyllis Fireman Charitable Foundation and grants to the Department of Ophthalmology at Tufts University School of Medicine from the Lions Eye Foundation and Research to Prevent Blindness.

References

1. Lim LS, Mitchell P, Seddon JM, Holz FG, Wong TY. Age-related macular degeneration. Lancet. 2012; 379(9827):1728–38. [PubMed: 22559899]
2. Bhutto I, Lutty G. Understanding age-related macular degeneration (AMD): relationships between the photoreceptor/retinal pigment epithelium/Bruch's membrane/choriocapillaris complex. Mol Aspects Med. 2012; 33(4):295–317. [PubMed: 22542780]
3. Mullins RF, Dewald AD, Streb LM, Wang K, Kuehn MH, Stone EM. Elevated membrane attack complex in human choroid with high risk complement factor H genotypes. Experimental eye research. 2011; 93(4):565–7. [PubMed: 21729696]
4. Haines JL, Hauser MA, Schmidt S, Scott WK, Olson LM, Gallins P, et al. Complement factor H variant increases the risk of age-related macular degeneration. Science. 2005; 308(5720):419–21. [PubMed: 15761120]
5. Davies A, Lachmann PJ. Membrane defence against complement lysis: the structure and biological properties of CD59. Immunol Res. 1993; 12(3):258–75. [PubMed: 7507156]
6. Kunchithapautham K, Bandyopadhyay M, Dahrouj M, Thurman JM, Rohrer B. Sublytic membrane-attack-complex activation and VEGF secretion in retinal pigment epithelial cells. Advances in experimental medicine and biology. 2012; 723:23–30. [PubMed: 22183311]
7. Halperin JA, Taratuska A, Nicholson-Weller A. Terminal complement complex C5b-9 stimulates mitogenesis in 3T3 cells. The Journal of clinical investigation. 1993; 91(5):1974–8. [PubMed: 8486768]
8. Kim DD, Song WC. Membrane complement regulatory proteins. Clin Immunol. 2006; 118(2-3): 127–36. [PubMed: 16338172]

9. Ebrahimi KB, Fijalkowski N, Cano M, Handa JT. Decreased membrane complement regulators in the retinal pigmented epithelium contributes to agerelated macular degeneration. The Journal of pathology. 2013; 229(5):729–42. [PubMed: 23097248]
10. Nishiguchi KM, Yasuma TR, Tomida D, Nakamura M, Ishikawa K, Kikuchi M, et al. C9-R95X polymorphism in patients with neovascular age-related macular degeneration. Invest Ophthalmol Vis Sci. 2012; 53(1):508–12. [PubMed: 22190594]
11. Clark SJ, Perveen R, Hakobyan S, Morgan BP, Sim RB, Bishop PN, et al. Impaired binding of the age-related macular degeneration-associated complement factor H 402H allotype to Bruch's membrane in human retina. J Biol Chem. 2010; 285(39):30192–202. [PubMed: 20660596]
12. Bengtsson E, Neame PJ, Heinegard D, Sommarin Y. The primary structure of a basic leucine-rich repeat protein, PRELP, found in connective tissues. J Biol Chem. 1995; 270(43):25639–44. [PubMed: 7592739]
13. Grover J, Chen XN, Korenberg JR, Recklies AD, Roughley PJ. The gene organization, chromosome location, and expression of a 55-kDa matrix protein (PRELP) of human articular cartilage. Genomics. 1996; 38(2):109–17. [PubMed: 8954791]
14. Happonen KE, Furst CM, Saxne T, Heinegard D, Blom AM. PRELP protein inhibits the formation of the complement membrane attack complex. J Biol Chem. 2012; 287(11):8092–100. [PubMed: 22267731]
15. Heinegard D, Larsson T, Sommarin Y, Franzen A, Paulsson M, Hedbom E. Two novel matrix proteins isolated from articular cartilage show wide distributions among connective tissues. J Biol Chem. 1986; 261(29):13866–72. [PubMed: 3759994]
16. Lewis M. PRELP, collagen, and a theory of Hutchinson-Gilford progeria. Ageing Res Rev. 2003; 2(1):95–105. [PubMed: 12437997]
17. Bengtsson E, Aspberg A, Heinegard D, Sommarin Y, Spillmann D. The aminoterminal part of PRELP binds to heparin and heparan sulfate. J Biol Chem. 2000; 275(52):40695–702. [PubMed: 11007795]
18. Bengtsson E, Morgelin M, Sasaki T, Timpl R, Heinegard D, Aspberg A. The leucine-rich repeat protein PRELP binds perlecan and collagens and may function as a basement membrane anchor. J Biol Chem. 2002; 277(17):15061–8. [PubMed: 11847210]
19. Tegla CA, Cudrici C, Patel S, Trippe R 3rd, Rus V, Niculescu F, et al. Membrane attack by complement: the assembly and biology of terminal complement complexes. Immunol Res. 2011; 51(1):45–60. [PubMed: 21850539]
20. Maller JB, Fagerness JA, Reynolds RC, Neale BM, Daly MJ, Seddon JM. Variation in complement factor 3 is associated with risk of age-related macular degeneration. Nat Genet. 2007; 39(10): 1200–1. [PubMed: 17767156]
21. Yates JR, Sepp T, Matharu BK, Khan JC, Thurlby DA, Shahid H, et al. Complement C3 variant and the risk of age-related macular degeneration. The New England journal of medicine. 2007; 357(6):553–61. [PubMed: 17634448]
22. Grossniklaus HE, Kang SJ, Berglin L. Animal models of choroidal and retinal neovascularization. Prog Retin Eye Res. 2010; 29(6):500–19. [PubMed: 20488255]
23. Pennesi ME, Neuringer M, Courtney RJ. Animal models of age related macular degeneration. Mol Aspects Med. 2012; 33(4):487–509. [PubMed: 22705444]
24. Askou AL, Pournaras JA, Pihlmann M, Svalgaard JD, Arsenijevic Y, Kostic C, et al. Reduction of choroidal neovascularization in mice by adeno-associated virus-delivered anti-vascular endothelial growth factor short hairpin RNA. J Gene Med. 2012; 14(11):632–41. [PubMed: 23080553]
25. Cashman SM, Ramo K, Kumar-Singh R. A non membrane-targeted human soluble CD59 attenuates choroidal neovascularization in a model of age related macular degeneration. PLoS One. 2011; 6(4):e19078. [PubMed: 21552568]
26. McClements ME, MacLaren RE. Gene therapy for retinal disease. Transl Res. 2013; 161(4):241–54. [PubMed: 23305707]
27. Hadders MA, Bubeck D, Roversi P, Hakobyan S, Forneris F, Morgan BP, et al. Assembly and regulation of the membrane attack complex based on structures of C5b6 and sC5b9. Cell reports. 2012; 1(3):200–7. [PubMed: 22832194]

28. Sparrow JR, Ueda K, Zhou J. Complement dysregulation in AMD: RPE-Bruch's membrane-choroid. Mol Aspects Med. 2012; 33(4):436–45. [PubMed: 22504022]
29. Anderson DH, Radeke MJ, Gallo NB, Chapin EA, Johnson PT, Curletti CR, et al. The pivotal role of the complement system in aging and age-related macular degeneration: hypothesis re-visited. Prog Retin Eye Res. 2010; 29(2):95–112. [PubMed: 19961953]
30. Ricklin D, Hajishengallis G, Yang K, Lambris JD. Complement: a key system for immune surveillance and homeostasis. Nat Immunol. 2010; 11(9):785–97. [PubMed: 20720586]
31. Ambati J, Atkinson JP, Gelfand BD. Immunology of age-related macular degeneration. Nature reviews. Immunology. 2013; 13(6):438–51.
32. Ambati J, Fowler BJ. Mechanisms of age-related macular degeneration. Neuron. 2012; 75(1):26–39. [PubMed: 22794258]
33. Yanai R, Thanos A, Connor KM. Complement involvement in neovascular ocular diseases. Advances in experimental medicine and biology. 2012; 946:161–83. [PubMed: 21948368]
34. Sottile J. Regulation of angiogenesis by extracellular matrix. Biochim Biophys Acta. 2004; 1654(1):13–22. [PubMed: 14984764]
35. Ricklin D. Manipulating the mediator: modulation of the alternative complement pathway C3 convertase in health, disease and therapy. Immunobiology. 2012; 217(11):1057–66. [PubMed: 22964231]
36. Bennett J, Ashtari M, Wellman J, Marshall KA, Cyckowski LL, Chung DC, et al. AAV2 gene therapy readministration in three adults with congenital blindness. Sci Transl Med. 2012; 4(120): 120ra15.
37. Aurnhammer C, Haase M, Muether N, Hausl M, Rauschhuber C, Huber I, et al. Universal real-time PCR for the detection and quantification of adeno-associated virus serotype 2-derived inverted terminal repeat sequences. Hum Gene Ther Methods. 2012; 23(1):18–28. [PubMed: 22428977]

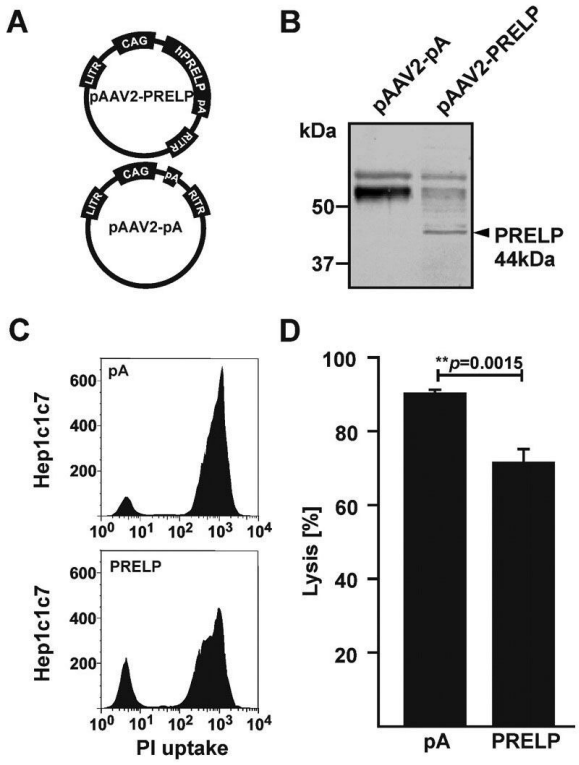

Figure 1. PRELP Inhibits Normal Human Serum Mediated Cell Lysis

(A) Schematic of pAAV2-PRELP containing the human PRELP cDNA regulated by the CAG promoter and negative control plasmid pAAV2-pA. **(B)** Western blot analyses of media/lysate from human ARPE-19 cells transfected with pAAV2-PRELP or pAAV2-pA, indicating a band of approximately 48 kDa associated with human PRELP specifically in media/lysate of pAAV2-PRELP transfected ARPE-19 cells. **(C)** Representative FACS-plots indicating the number of Hepa-1c1c7 cells taking up propidium iodide following incubation in 1.5% normal human serum (NHS) preconditioned with media from human ARPE-19 cells transfected with pAAV2-PRELP or pAAV2-pA. **(D)** Quantification of FACS-lysis assays. PRELP reduced cell lysis by 18.74±3.95% (mean value±SEM; ***p=0.0015*; n=5). CAG: chicken β-actin promoter with CMV enhancer; LITR/RITR: left/right AAV inverted terminal repeat; pA: poly-adenylation sequence.

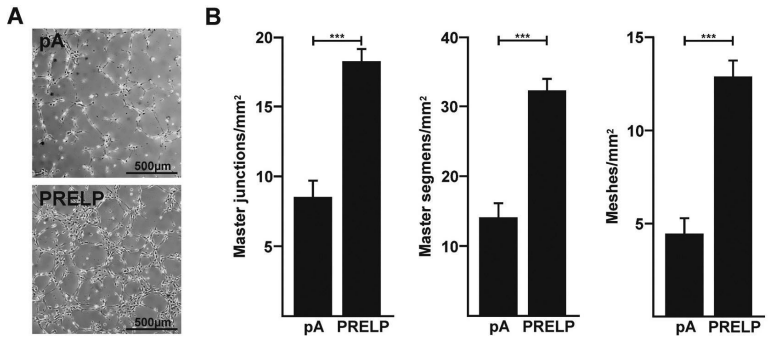

Figure 2. Human PRELP Promotes Formation of Tubes by HUVECs

(A) Representative phase contrast images of tubes formed by HUVECs incubated in pAAV2-pA (pA) or pAAV2-PRELP (PRELP) conditioned media. **(B)** Graphical plot of mean values ± SEM of resulting master junctions, master segments and master meshes in HUVECs incubated in pA or PRELP conditioned media. PRELP significantly increased the numbers of master junctions by 2.1-fold (***$p<0.0001$), master segments by 2.3-fold (***$p<0.0001$) and meshes by 2.9-fold for (***$p<0.0001$). Studies were performed 4 times in triplicate (n=12).

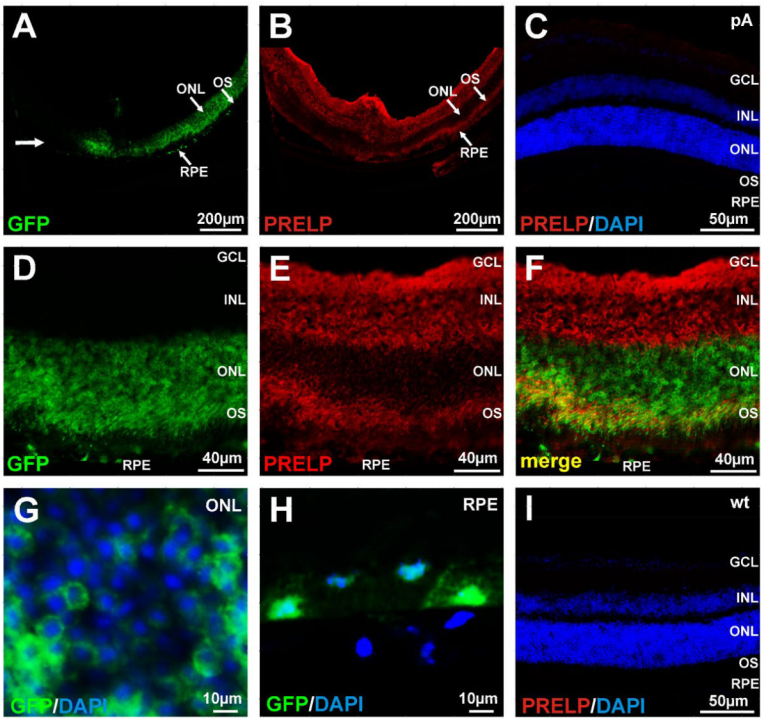

Figure 3. AAV2/8 Mediated Expression of PRELP

In order to distinguish virus tropism from that of localization of PRELP, AAV2/8-PRELP or AAV2/8-pA was spiked with AAV2/8-GFP. **(A)** Unidirectional distribution of GFP in the ONL and RPE along the line of the injection (bold arrow) following subretinal injection of AAV2/8-PRELP + AAV2/8-GFP in mice. **(B)** Cy3 (PRELP) staining in the inner retina and outer segments of photoreceptors. **(C)** Cy3 labeled section of an AAV2/8-pA injected eye. Nuclei are counterstained with DAPI. **(D)** Higher magnification of retina from mice following subretinal injection of AAV2/8-PRELP spiked with AAV2/8-GFP. GFP is present in the ONL, outer segments and RPE. **(E)** Human PRELP is exclusively present in the inner retina and outer segments with a weak signal in the RPE. **(F)** Merged images of GFP and Cy3 (PRELP) indicating some regions of overlap (yellow) and distinct regions of expression for GFP and PRELP, indicative of PRELP being synthesized in the photoreceptors and RPE but being secreted and localizing to the inner retina and photoreceptor outer segments. **(G)** Higher power images of GFP/DAPI overlays from the ONL and **(H)** RPE. **(I)** Cy3 labeled section of an uninjected wt eye. Nuclei are counterstained with DAPI. RPE; retinal pigment epithelum, OS; photoreceptor outer segments, ONL; outer nuclear layer, INL; inner nuclear layer, GCL; ganglion cell layer.

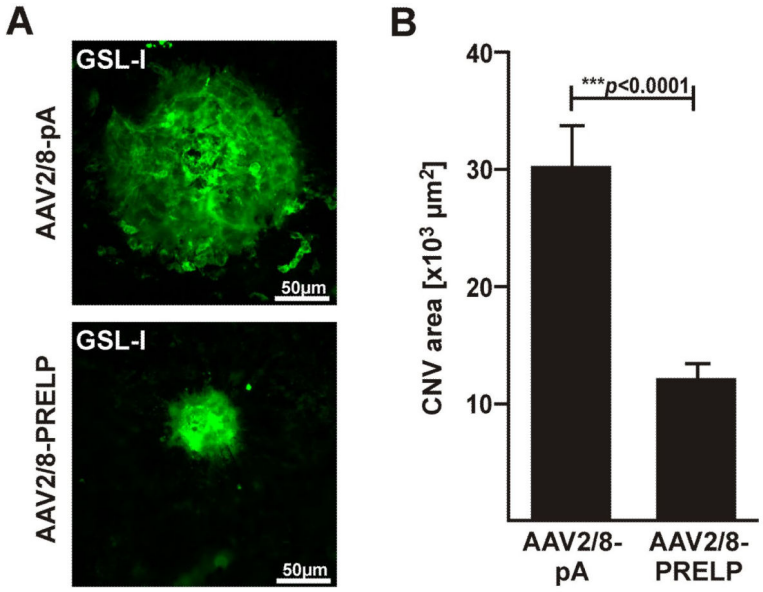

Figure 4. Human PRELP Attenuates Choroidal Neovascularization in Mice

(A) Representative micrographs of FITC·GSL-1 stained laser-induced CNV spots from eyes injected with AAV2/8-pA or AAV2/8-PRELP one week post laser. **(B)** Graphical plot of mean values ± SEM of CNV area in AAV2/8-pA and AAV2/8-Prelp injected eyes. Average CNV area was significantly reduced by 60.0±13.1% (***$p<0.0001$) in AAV2/8-PRELP injected eyes. Studies were performed twice with 5 mice in each group (n=10 mice/ 20 eyes; AAV2/8-pA: 61 laser spots, AAV2/8-Prelp: 55 laser spots).

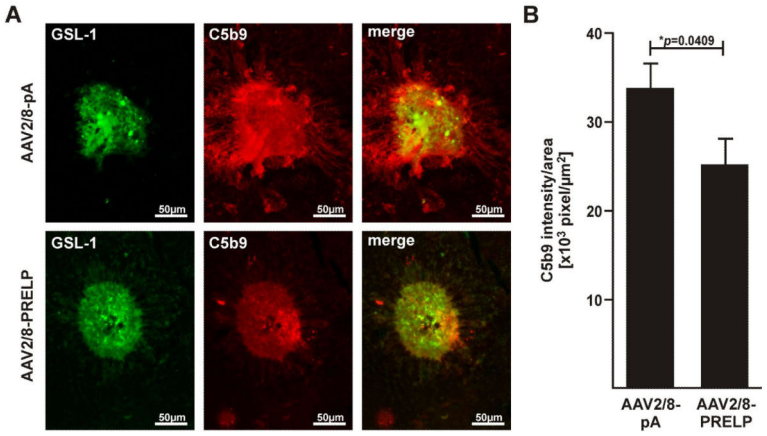

Figure 5. Human PRELP Attenuates Formation of Membrane Attack Complex in Mice

(A) Representative micrographs of C5b9 labeled laser-induced CNV spots from eyes injected with AAV2/8-pA or AAV2/8-PRELP 7 days post laser. Overlays of GSL-1 and C5b9 stainings of equal sized CNV spots indicating MAC deposition confined within borders of CNV in AAV2/8-PRELP infected eyes, but spread beyond the CNV area in the negative controls. Note that there was variability in GSL-1 staining between laser spots and this was overcome by use of a relatively large sample size. In the above figure, two spots of roughly equivalent GSL-1 staining were selected in order to demonstrate the corresponding differences in C5b9 staining. **(B)** Graphical plot of mean values±SEM of C5b9 intesity/area ratios in AAV2/8-pA and AAV2/8-Prelp injected eyes. Average ratio was significantly reduced by 25.5±12.3% (*$p=0.0409$) in AAV2/8-PRELP infected eyes. Studies were performed twice with 5 mice in each group (n=10 mice/ 20 eyes; AAV2/8-pA: 61 laser spots, AAV2/8-Prelp: 55 laser spots).